# Revista Sul-Americana de Engenharia Estrutural



# Modeling of the flexural tensile strength of concrete made with recycled aggregates from CDW

Magno Teixeira Mota<sup>1</sup>, Marcelo Pedreira da Silva<sup>1</sup>, Anderson de Souza Matos Gádea<sup>1</sup>, Mônica Batista Leite<sup>1</sup>, Koji de Jesus Nagahama<sup>1\*</sup>

#### **Abstract**

The increasing scarcity of natural resources used by the building industry and the environmental problems caused by construction and demolition waste (CDW) have motivated the use of aggregates produced from those waste in the composition of concretes. Several studies have shown that, in general, the concrete produced with such aggregates, when compared with the conventional, displays changes in important engineering properties, such as reduction of the compressive strength and modulus of elasticity. Nevertheless, some experimental studies have indicated that it is possible to use it in the production of structural elements with satisfactory mechanical behavior. Before this scenario, there appears the necessity to evaluate the possibility of prediction of the mechanical behavior that concrete. In accordance with this need, this paper aims to reproduce the results of flexural tensile strength of concretes containing CDW recycled aggregates, through numerical modeling based in the Finite Element Method (FEM), performed with the DIANA® software. The results indicate that it is possible to obtain numerical models that estimate satisfactorily the flexural tensile strength those concretes.

Keywords: numerical simulation, FEM, flexural tensile strength, recycled aggregates, CDW.

Av. Transnordestina, s/n, Novo Horizonte, ZIP 44036-900, Feira de Santana, Bahia, Brazil.

<sup>&</sup>lt;sup>1</sup> State University of Feira de Santana – UEFS.

<sup>\*</sup> Corresponding author: koji@uefs.br

# 1 Introduction

Due to the environmental impacts caused by *CDW* and the increasing scarcity of natural resources used by the civil engineering construction, several studies have been carried out with aim to evaluate the use of recycled aggregates from *CDW* in concrete. According to Cabral (2007), the *CDW* generated in Brazil is composed, on average, by 65% of mineral material (concrete, mortar and ceramic material), 13% of wood, 8% of plastic and 14% of other materials, a composition that permits, after processing, that the *CDW* be used in the production of concretes.

The use of recycled aggregates requires a systematic study of its properties, such as specific density, water absorption, granulometric distribution, resistance, hardness, shape of the aggregates and chemical composition Leite (2009). Variations in these properties affect the physical and mechanical properties of the recycled concrete (Corinaldesi *et al.* 2009, Tam *et al.* 2008 and Tam and Tam 2008).

Recent studies show the influence of recycled aggregates in the mechanical behavior of concrete. Eguchi *et al.* (2007) developed a method for the production of recycled concrete at low cost. In the study of the mechanical properties of concrete containing recycled coarse aggregate, these authors noted a decrease of the compressive strength and modulus of elasticity with an increase in the content of recycled aggregates.

As to axial tensile strength, several studies (Bairagi *et al.* 1993, Gómes-Saberón 2002 and Kumutha *et al.* 2010) also verified a decrease in the values obtained for this property in recycled concretes when compared with the results of conventional concretes, mainly when the natural coarse aggregates are substituted by recycled ones. Nevertheless, Leite (2001) and Larrañga (2004) observed that the relationship between the axial tensile strength and compressive strength ( $f_t/f_c$ ) of the recycled concrete is higher than the relationships generally known for conventional concretes.

Li (2009) evaluated the influence of recycled aggregates content on behavior of reinforced concrete beams under flexure. In compare with the conventional concrete beam, the recycled concrete beam presented a decrease of rigidity and an increase of 10 to 24% in the central deflection.

Parallel to experimental studies, numerical analyses are necessary to evaluate the possibility of predicting the structural behavior of recycled concrete. Since require significant amount of experimental results to be validated, the researches on numerical modeling of constructive elements of recycled concrete are still in initial phase. Can be mentioned the research carried out by Xiao *et al.* (2009), in which a non-linear numerical model based on the *FEM* was used to analyze the behavior of frame joints of recycled concrete submitted to seismic loads. The results obtained were compatible with the experimental tests, taking into account, among other variables, the bond behavior between the recycled concrete and the steel bars.

In order to contribute to the studies on the mechanical behavior of concrete containing recycled aggregates from CDW, this paper aims to determine the flexural tensile strength of this composite through numerical modeling by FEM. For this purpose, a flexural beam model was developed with the DIANA® software by using parameters obtained in axial compressive test and direct tension test in specimens of recycled concrete.

#### 2 Concrete under uniaxial tension

The understanding of the flexural behavior of the plain concrete is directly related to the knowledge of the composite state of stresses to the which its cross-section is submitted. In this context, the responses of the concrete to contrary solicitations in this section (compressive and tensile stresses) have distinct characteristics regarding the degradation of this material. Analyzing the development of cracks in both cases, it can be observed that the velocity of propagation of the same in the part submitted to tensile stress of this section is substantially higher than in the part submitted to compressive stress. This behavior arises, according to Mehta and Monteiro (2008), due to the tendency of the state of tensile stress to interrupt cracks much less often than the states of compressive stress, making the stable interval of tensile cracks propagation be lot shorter. Thus, in bending of plain concrete, the maximum tensile stress determines the onset of its rupture.

The studies on tensile cracks of concrete were started in the mid 20<sup>th</sup> century by using an method analogous to the investigations on the compressive behavior carried out by Gonnerman and Shuman *apud* Hordijk (1991). In the 1960s, Rüsch and Hilsdorf *apud* Hordijk (1991) realized extensive studies on the post-peak behavior in direct tension tests and detected a descending branch in the stress-deformation relationship. Such investigations allowed to conclude that concrete, when submitted to those tests, can present rupture form depending on the loading conditions. In tests where the loading is done under load control,

the rupture of the samples happens suddenly (Figure 1a). But, when submitted to displacement control, with adequate rigidity of the test machine, it is possible to observe a descending branch after the rupture as can be observed in Figure 1b. This branch is known as softening.

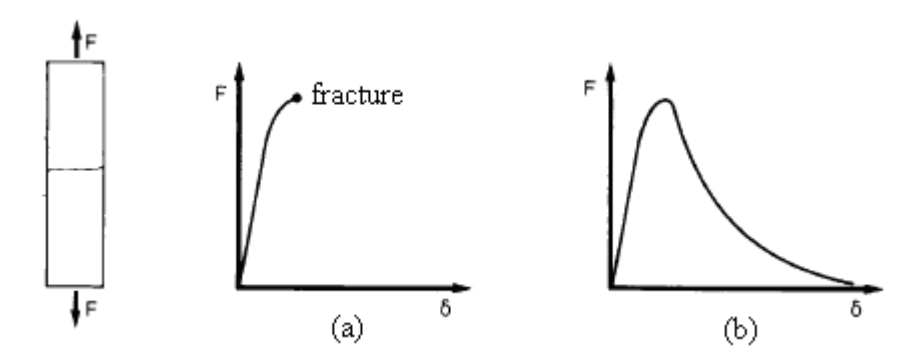
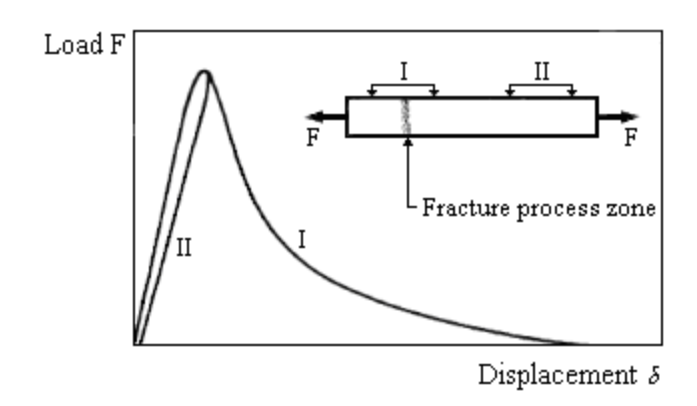


Figure 1 Direct tension test: (a) load control; (b) displacement control (Hordijk 1991).

The softening, also observed experimentally by Gopalaratman and Shah (1985), begins when the tensile strength of concrete is reached in a narrow band called fracture process zone (Figure 2) in which develop localized micro cracks and later an macro crack. This zone occurs in the weakest section of the specimen and can be understood through the fictitious crack model proposed for fracture of concrete by Hillerborg at al. (1976). If the fracture process zone develops within the stretch of the specimen in which the displacement is measured, will be observed a descending branch in the post-peak behavior of the load-displacement diagram (line I of Figure 2). In this stretch, the load that can be transferred decreases gradually with the increase of the displacement. Outside of the fracture process zone, a displacement measurer will detect the unloading of the concrete (line II of Figure 2).



**Figure 2** Load-displacement relation for a specimen under uniaxial tensile loading (Hordijk 1991).

# 2.1 Test Procedures to Determine the Tensile Strength of Concrete

The tensile strength of the concrete can be evaluated through three procedures: direct tension test, split-tension test according to Brazilian Standard NBR 7222 (1994)or flexural test according to Brazilian Standard NBR 12142 (1994). Of these, the method of direct tension is the one that shows the higher complexity in the test configuration, particularly because of the difficulty to ensure the necessary adherence between the specimen and the equipment without causing undue stress concentrations. On the other hand, the results obtained with the indirect methods show overestimated values of resistance when compared to the results of direct tension tests.

According to Mehta and Monteiro (2008), the tensile strength obtained with the split-tension test is approximately 10 to 15% higher than the one observed in direct tension test. In the flexural test, the tensile strength is overestimated in 50 to 100%. In this test, the equation for the calculus of the tensile strength considers the relationship stress-strain in all cross-section of the beam as being linear. This increases the tensile strength calculated. The form of applying the tensile stress also contributes for this result. In the direct tension, all the volume of the specimen is submitted to applied stress, while in flexural test the stress is applied in a small volume of concrete near to the inferior part of the beam. Another important characteristic of the flexural test consists in the fact that the specimen rupture occurs in the central third of the same, as observed in Figure 3.

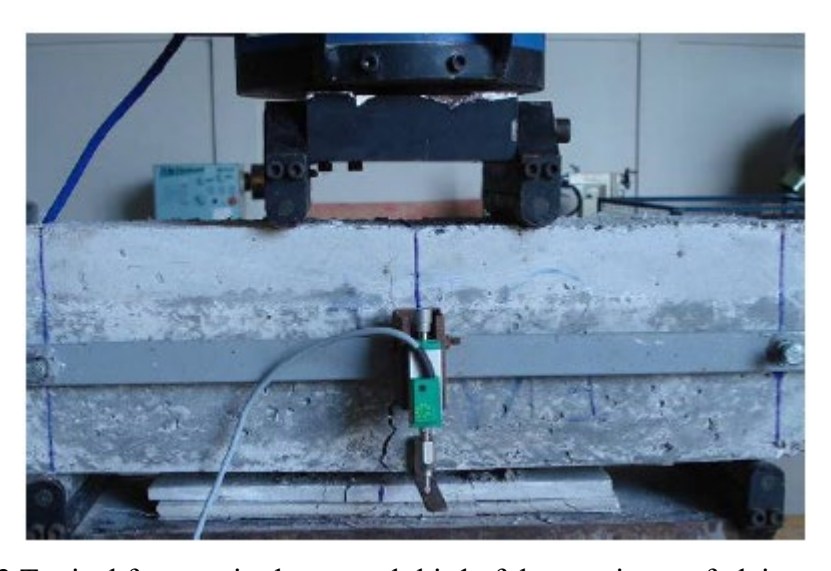


**Figure 3** Typical fracture in the central third of the specimen of plain concrete in flexural test (Santiago 2008).

# 3 Smeared crack models

Tables and figures must be numbered consecutively and referred to in the text. All tables and figures must have captions and should accompany the manuscript, but should not be included within the text. They are shown on separate pages at the end of this manuscript.

The cracking modeling is a complex procedure since the cracks are associated to discontinuities in the field of displacements. For numerical simulation, via FEM, of concrete structures subject to cracking, the smeared crack concept is widely used by researchers. In this concept, the cracked material is regarded as continuous and the discontinuity in the field of displacement caused by the cracking is spreaded along the finite element. In that case, the crack is represented by change in the constitutive law of the material, maintaining itself unchanged the finite element mesh (Rots 1988 and Menin *et al.* 2009). In the smeared crack models, can be utilized three crack concepts: fixed crack, rotating crack or multi-directional fixed crack.

In the fixed crack model, the orientation of the cracks is kept constant during the loading. In the rotating crack model, the principal axes of orthotropic rotate coaxially with the principal strains during crack propagation in the material Feenstra (1991). The multi-directional fixed crack model is an intermediate model that allows the opening of several cracks in a same point. In this study, this last model was used to represent the cracks resulting from the flexural behavior of the specimens.

# 3.1 Multi-directional fixed crack model

According to Menin *et al.* (2009), the multi-directional fixed crack model allows to describe a larger variety of real situations since associates the behavior of the fixed and rotational crack models, besides to enable the adoption a tensile behavior for concrete and to allow the adjustment of the shear stiffness by means of a parameter named shear retention factor ( $\beta$ ). For this study, was adopted  $\beta = 0.2$ , as recommended (Menin *et al.* 2009). The tension cutoff criteria used was the constant stress cut-off (Figure 4) through which the onset of the cracking occurs when the principal tensile stress exceeds the tensile strength of concrete.

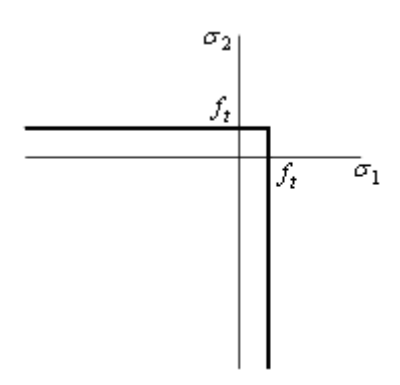


Figure 4 Constant stress cut-off (DIANA 2005).

For the multi-directional fixed crack model, the DIANA® software enables, in general, the applying of four tension softening relations: brittle, linear, multilinear and nonlinear. In this study, were used the brittle and nonlinear models. In the brittle model (Figure 5a), the tensile stress reduces to zero after reaching the tensile strength ( $f_t$ ) of the material. The nonlinear model was the one proposed by Hordijk (1991), shown in Figure 5b, based on energetic criteria associated to the Fracture Mechanics and with softening diagram described by Equation (1).

$$\frac{\sigma_{t}^{cr}}{f_{t}} = \begin{cases} \left(1 + \left(c_{1} \frac{\varepsilon^{cr}}{\varepsilon_{u}^{cr}}\right)^{3}\right) \exp\left(-c_{1} \frac{\varepsilon^{cr}}{\varepsilon_{u}^{cr}}\right) - \frac{\varepsilon^{cr}}{\varepsilon_{u}^{cr}} \left(1 + c_{1}^{3}\right) \exp\left(-c_{2}\right) \rightarrow 0 < \varepsilon^{cr} < \varepsilon_{u}^{cr} \\ 0 \rightarrow \varepsilon_{u}^{cr} < \varepsilon^{cr} < \infty \end{cases} \tag{1}$$

where  $\sigma_t^{\alpha}$  e  $\varepsilon^{\alpha}$  are, respectively, the crack normal stress and the crack normal strain,  $c_1$  as well as  $c_2$  are dimensionless adjustment parameters whose values recommended by DIANA® software are respectively 3.00 and 6.93 [24].

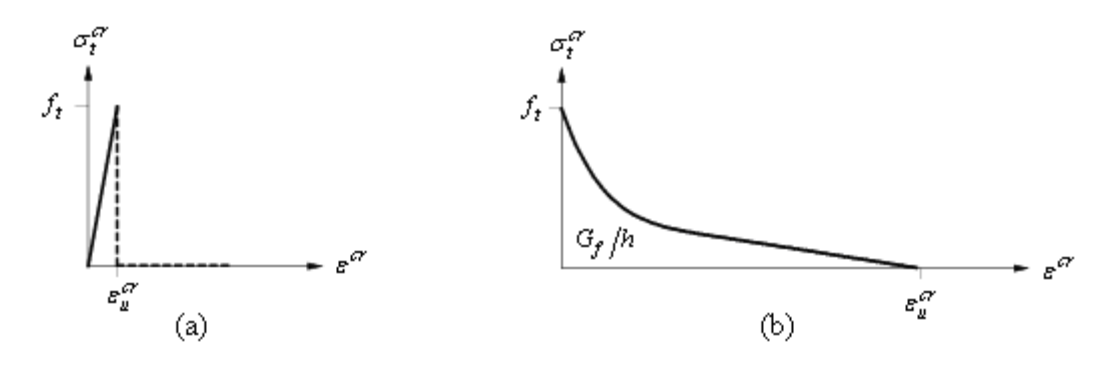


Figure 5 Tension softening: (a) brittle model; (b) softening diagram (Hordijk 1991).

Revista Sul-Americana de Engenharia Estrutural, Passo Fundo, V. 19 n. 1, p. 51-68, jan./abr. 2022

Regarding the model by Hordijk, it is important to observe that the area under the curve of Figure 5b is equivalent to the energy necessary to open a crack unit in direct tension, determined by means of relation  $G_f/h$ , where  $G_f$  is the fracture energy and h is the width of the fracture process zone or crack bandwidth. The fracture energy according to CEB-FIP Model Code (1990) can be obtained using Equation (2).

$$G_f = G_{f0} \left( \frac{f_{cm}}{f_{cm}} \right)^{0.7} \tag{2}$$

where  $f_{cm} = f_{ck} + \Delta f$ , being  $f_{ck}$  the characteristic compressive strength and  $\Delta f = 8MPa$ ,  $f_{cm} = 10MPa$  and the parameter  $G_{f0}$  depends on the maximum aggregate size  $(d_a)$  and can be determined from Table 1.

Table 1 Values of G<sub>f0</sub>

d <sub>a</sub> (mm)	$G_{f\theta}$ (N/m)
8	25
16	30
32	58

The crack bandwidth can be calculated by means of Equation (3) proposed by Bazant and Oh (1993).

$$h = n_a \cdot d_a \tag{3}$$

where  $n_a$  is an empirical constant whose value suggested is 3 for concrete and 5 for rock.

# 4 Formulation of the numerical model

In this study, were used results obtained by Leite (2009) relating to direct tension test in six concrete mixtures with ratio water-cement equal to 0.45: REF (reference concrete without recycled aggregates), 50AMR (concrete with 50% of recycled fine aggregates), 100AMR (concrete with 100% recycled fine aggregates) 50 AGR (concrete with 50% of recycled coarse aggregates), 100AGR (concrete with 100% recycled coarse aggregates) and 50AMR-AGR (concrete with 50% of recycled fine aggregates and 50% of recycled coarse aggregates). For each mixture, six samples were produced. The CDW used was basically

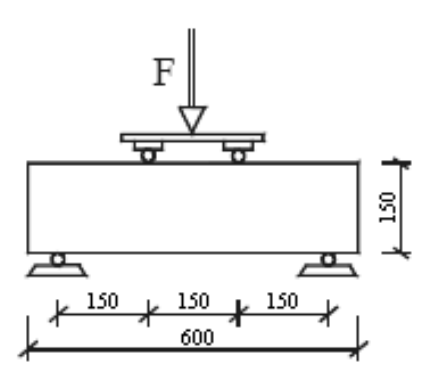
composed by 54.5% of mortar, 26% of ceramic material, 16.4% of concrete and 1.3% of rock.

Table 2 shows the experimental parameters obtained by Leite (2009) that are used in this study: direct tensile strength ( $\mathbf{f_t}$ ), uniaxial compressive strength ( $\mathbf{f_c}$ ), modulus of elasticity ( $\mathbf{E}$ ) and Poisson's coefficient ( $\mathbf{v}$ ). The geometry and the loading conditions of the specimens were the ones recommended by ISO 4013 (1978), also adopted by the Brazilian Standard NBR 12142 (1994).

Table 2 Experimental data used in this study

Concrete	f <sub>t</sub> (MPa)	fc (MPa)	E (GPa)	
REF	2.5	46.6	34.60	0.21
50AMR	2.1	39.2	28.70	0.20
100AMR	1.8	30.3	23.80	0.21
50AGR	2.6	36.0	29.00	0.20
100AGR	2.3	28.4	24.80	0.19
50AMR-AGR	2.0	30.8	23.30	0.21

The dimensions of the specimens were  $150 \times 150 \times 600$  mm and the test conditions are detailed in Figure 6.



**Figure 6** Dimensions (mm) and loading conditions of the specimens used in the numerical simulations.

For the numerical simulation with the DIANA® software, was carried out a two-dimensional structural static analysis with displacement control. The mesh used in the numerical model was determined based on a study of convergence in which it was defined how adequate a discretization of 12×48 elements. So, the dimensions of each element were 12.5×12.5 mm. The finite element used was the Q8MEM, which is a plane stress element, quadrilateral, with four nodes and based on quadratic interpolation and Gauss integration.

Leite [2] did not perform flexural test, therefore, to make possible the evaluation of the numerical results, this parameter was estimated theoretically through the Equation (4) proposed by the Model Code 1990 (1991).

$$f_{t,ff}^{\text{theo}} = f_t \frac{1 + 1.5 (h_1/h_0)^{0.7}}{1.5 (h_1/h_0)^{0.7}}$$
(4)

where  $f_{t,fl}^{theo}$  is the theoretical value of flexural tensile strength (MPa) following itself the recommendations of ISO 4013 [27],  $f_t$  is the uniaxial tensile strength (MPa),  $f_t$  is the depth of beam (mm) e  $f_t$  = 100 mm. Table 3 shows the values of  $f_{t,fl}^{theo}$  for analyzed mixtures. The value of flexural tensile strength obtained with numerical model ( $f_{t,fl}^{num}$ ) was determined via the Equation (5).

$$f_{t,f}^{num} = \frac{M \cdot y}{1} \tag{5}$$

where  $M = F \cdot I/3$  is the bending moment in central section of specimen, being F the maximum load in one of the supports and I the distance between the supports. Parameter I is the moment of inertia of the cross-section of specimen and y = I/6.

Table 3 Values of  $f_{t,f}^{theo}$ 

Concrete	$f_t$ (MPa)	$f_{t,ff}^{theo}$ (MPa)
REF	2.5	3.76
50AMR	2.1	3.15
100AMR	1.8	2.70
50AGR	2.6	3.91
100AGR	2.3	3.45
50AMR-AGR	2.0	3.00

In the research carried out by Leite (2009), the maximum aggregate size was 9.5 mm for natural aggregates and 19 mm for recycled aggregates. Given these values, Table 4 shows the crack bandwidth calculated by Equation (3) for the analyzed mixtures. The fracture

energy of the numerical models was obtained in two ways: by using Equation (2) and performing an inverse analysis with the softening diagram of Hordijk (1991).

Table 4 Values of crack bandwidth for the analyzed mixtures

Concrete	h (mm)
REF	28.5
50AMR	28.5
100AMR	28.5
50AGR	57.0
100AGR	57.0
50AMR-AGR	57.0

# 4.1 Determination of the fracture energy through the softening diagram of Hordijk

As shown in Figure 5b, the area below the softening diagram of Hordijk model depends on four parameters: fracture energy, crack bandwidth, tensile strength and ultimate crack strain  $(\varepsilon_u^{\alpha})$ . To reach an efficient calibration of the fracture energy, it is necessary, first, to know the existing relationship between these parameters. In general, the relationship between tensile strength and deformation in the cracked concrete,  $\sigma_t^{\alpha}$  and  $\varepsilon^{\alpha}$ , respectively, is established as

$$\sigma_t^{\alpha}(\varepsilon^{\alpha}) = f_t \cdot y \left( \frac{\varepsilon^{\alpha}}{\varepsilon_u^{\alpha}} \right) \tag{6}$$

where  $y\left(\frac{\varepsilon^{\alpha}}{\varepsilon_{u}^{\alpha}}\right)$  is the function that defines the shape of the softening.

Based on the calculus of the area below the softening curve, the fracture energy can be defined by

$$G_{f} = h \int_{\varepsilon^{\alpha} = 0}^{\varepsilon^{\alpha} = \varepsilon_{u}^{\alpha}} \sigma_{t}^{\alpha}(\varepsilon^{\alpha}) d\varepsilon^{\alpha}$$
 (7)

Substituting Equation (6) into Equation (7) leads to

$$G_{f} = h f_{t} \int_{\varepsilon^{\alpha} = 0}^{\varepsilon^{\alpha} = \varepsilon_{u}^{\alpha}} y \left( \frac{\varepsilon^{\alpha}}{\varepsilon_{u}^{\alpha}} \right) d\varepsilon^{\alpha}$$
(8)

With the variable change defined in Equation (9) it is obtained Equation (11).

$$\mathbf{X} = \frac{\varepsilon^{\mathbf{a}}}{\varepsilon_{u}^{\mathbf{a}}} \tag{9}$$

$$d\varepsilon^{\alpha} = \varepsilon_{\mu}^{\alpha} d\mathbf{x} \tag{10}$$

$$G_{f} = h f_{t} \left( \int_{x=0}^{x=1} y(x) dx \right) \varepsilon_{u}^{\sigma}$$
 (11)

The Equation (11) can be rewritten as

$$\varepsilon_{u}^{\sigma} = \frac{1}{\alpha} \cdot \frac{G_{f}}{h f_{t}} \tag{12}$$

where the value of  $\alpha$  depends of the adopted softening diagram. Since the softening diagram of Hordijk (1991) is defined by Equation (1), in this work, the value of  $\alpha$  is given by

$$\alpha = \int_{x=0}^{x=1} y(x) dx = \int_{x=0}^{x=1} \left( 1 + (c_1 x)^3 \right) \exp(-c_2 x) - x \left( 1 + c_1^3 \right) \exp(-c_2) dx$$
 (13)

which results in  $\alpha = 0.195$  for  $c_1 = 3$  and  $c_2 = 6.93$ . Thus, the Equation (12) becomes

$$\varepsilon_u^{\sigma} = 5.136 \frac{G_f}{h f_t} \tag{14}$$

Through the Equation (14), was performed the calibration of the fracture energy of the numerical models with the reference concrete (REF). Observing that the crack bandwidth and tensile strength have definite values, the fracture energy was varied until the flexural tensile strength of the numerical model came as close as possible to the expected value calculated by Equation (4). The ultimate crack strain obtained in this calibration, equal to **0.01145**, was fixed for the modeling of the other concretes which had the fracture energy estimated in a fast way, depending only on the uniaxial tensile strength of the same.

# 5 Results and discussion

The results obtained with the applying of brittle model (Figure 5a) are presented in Table 5. The parameters shown in this table are: theoretical flexural tensile strength, numerical flexural tensile strength and the variation between numerical and theoretical values. It can be observed that the applying of brittle model significantly underestimates the flexural tensile strength, with results, on average, approximately 36% lower than the values theoretically expected. Such results indicate that it is necessary to consider the softening

branch in tension for to obtain values of flexural tensile strength compatible with those expected.

**Table 5** Results obtained with the brittle model

Concrete	$f_{t,ff}^{theo}$	$f_{t,fl}^{\;num}$	Variation
	(MPa)	(MPa)	(%)
REF	3.76	2.42	-35.5
50AMR	3.15	2.01	-36.3
100AMR	2.70	1.75	-35.3
50AGR	3.91	2.46	-37.1
100AGR	3.45	2.19	-36.6
50AMR-AGR	3.00	1.89	-37.2

Table 6 shows the results obtained with the softening diagram of Hordijk with the fracture energy estimated by Equation (2). The parameters shown in this table are: fracture energy, numerical flexural tensile strength and the variation between numerical and theoretical values of flexural tensile strength. It can be verified that the values of flexural tensile strength of the numerical models present a significant increase compared to the ones shown in Table 4. However, comparing these with the expected values, large variations can be observed mainly for the concretes produced with recycled coarse aggregates (50AGR, 100AGR and 50 AMR-AGR). These results can be explained observing that Equation (2) does not consider the uniaxial tensile strength of the concrete, which, in the flexural tests of plain concretes, has direct influence upon the results because determines onset of the specimen rupture besides being the only variable parameter in Equation (4).

**Table 6** Results obtained using the softening diagram of Hordijk with fracture energy determined by Equation (2)

Concrete	G <sub>f</sub> (N/m)	$f_{t,fl}^{num}$ (MPa)	Variation (%)
REF	85.11	3.45	-8.2
50AMR	76.87	2.93	-7.1
100AMR	66.41	2.46	-8.9
50AGR	99.44	3.13	-20.0
100AGR	87.08	2.69	-22.0

50AMR-AGR	91.06	2.49	-17.1
-----------	-------	------	-------

Table 7 shows the results obtained with fracture energy estimated by Equation (14) after calibration with the REF concrete. In this case, also was used the softening diagram of Hordijk. Due to calibration performed with REF concrete, the variation between  $f_{t,fl}^{num}$  and  $f_{t,fl}^{theo}$  for this concrete was only 0.1%, in modulus. The results for the other concretes indicate that the determination of the fracture energy through the softening diagram of Hordijk was, in general, efficient in determining the flexural tensile strength of the recycled concretes, presenting maximum variation, in modulus, equal to 6.5% when compared with the expected value. Observing the experimental data of REF, 50AGR and 100AGR concretes in Table 2, it can be noted that the substitution of natural coarse aggregates by recycled coarse aggregates causes a marked reduction in the modulus of elasticity and a small variation in the uniaxial tensile strength, making it difficult to predict the results via numerical modeling. Thus, the variation, in modulus, of 6.5% between  $f_{t,fl}^{num}$  and  $f_{t,fl}^{theo}$  for the 100AGR concrete can be considered satisfactory, since the same presents the most unfavorable modeling situation.

**Table 7** Results obtained using the softening diagram of Hordijk with fracture energy determined by Equation (14)

Concrete	$G_f$ (N/m)	f <sub>t,ff</sub> <sup>num</sup> (MPa)	Variation (%)
REF	158.8	3.75	-0.1
50AMR	133.4	3.17	0.6
100AMR	114.4	2.67	-1.2
50AGR	330.4	3.76	-3.9
100AGR	292.3	3.23	-6.5
50AMR-AGR	254.1	2.92	-2.7

Figure 7 shows the normal stress distributions before the appearance of cracks (Figure 7a) and during the rupture of the numerical model of the REF concrete obtained with the softening diagram of Hordijk, with fracture energy estimated by Equation (14). Similar

configurations were obtained for the other concretes as well as for the models in which the fractural energy was determined by Equation (2).

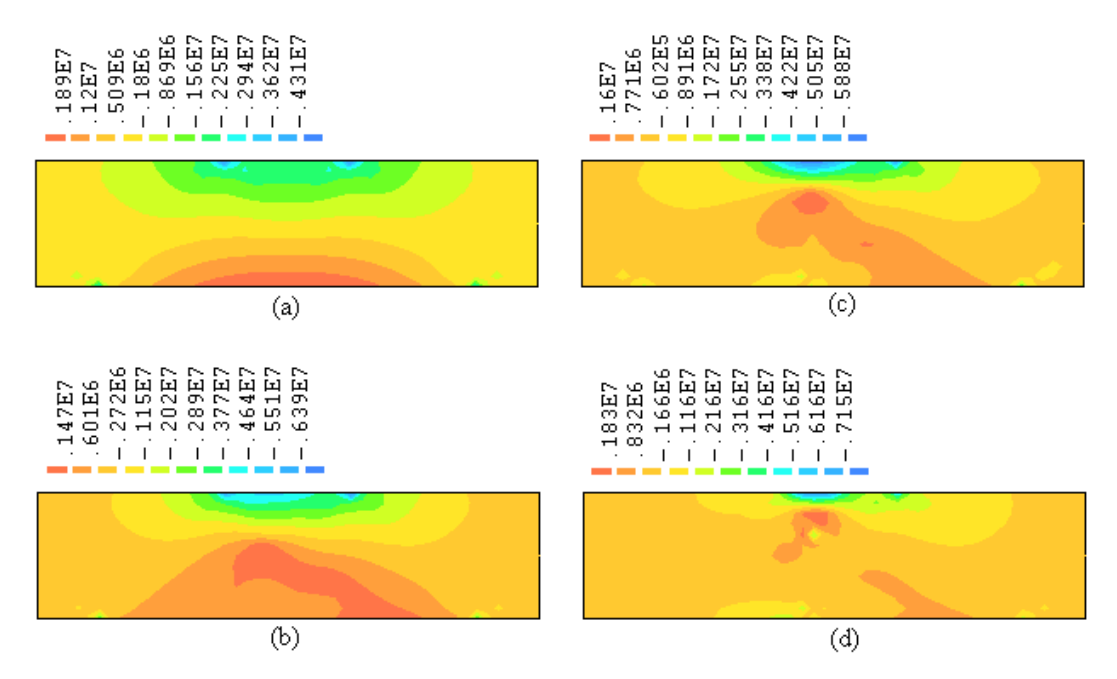


**Figure 7** Normal stresses (Pa) to cross-section: (a) before the appearance of cracks; (b), (c), (d) during the failure of the numerical model.

The stress distributions observed in Figure 7 are consistent with the condition of pure bending to which the central third of the specimen is submitted, with the rupture happening in this stretch, as can be verified in experimental tests (Figure 3). Furthermore, it can also be observed that the rupture occurs gradually due to the adoption of the tension softening diagram.

#### 6 Conclusions

The use of the brittle model underestimated considerably the flexural tensile strength of concretes, were obtained values, on average, 36% below those expected (Table 5). This result indicates that the softening behavior in tension must be considered in order to obtain satisfactory results.

Using the softening diagram of Hordijk, with the fracture energy determined by Equation (2) proposed by Model Code 1990 (1991), was observed a significant increase in the flexural tensile strength compared to the results obtained with the brittle model. However, considerable variations still were observed between  $f_{t,n}^{num}$  and  $f_{t,n}^{theo}$ , mainly for the concretes produced with recycled coarse aggregates (Table 6). On the other hand, the use of the

softening diagram of Hordijk with the fracture energy obtained from this diagram was efficient in the determination of the flexural tensile strength of recycled concretes. The maximum variation, in modulus, between  $f_{t,n}^{num}$  and  $f_{t,n}^{theo}$ , was 6.5% (Table 7), being that four of the five analyzed results showed variations inferior to 4% indicating a satisfactory predictability of this parameter.

The numerical models obtained from the softening diagram of Hordijk showed normal stress distributions consistent with the test configuration (Figure 7), with the rupture occurring in the central third of the model, as verified in the experiments (Figure 3).

The results indicated that, even though the recycled aggregates cause alterations in the mechanical properties of the concrete, the flexural tensile strength of recycled concretes can be satisfactorily estimated using parameters obtained in experimental tests, such as maximum aggregate size, uniaxial tensile strength, modulus of elasticity and Poisson's coefficient.

# 7 Acknowledgements

The authors thank the CAPES and CNPq for their research support.

#### 8 References

Cabral A.E.B., (2007). Mechanical properties and durability modeling of recycled aggregates concrete, considering the construction and demolition waste variability. Doctoral thesis. University of São Paulo, School of Engineering at São Carlos, 280 p. (in Portuguese).

Leite M.B., (2009). Evaluation of the stress-strain behavior of recycled concrete subjected to axial compression and direct tension. Dissertation for career progression. State University of Feira de Santana, Feira de Santana, 65 p. (in Portuguese).

Corinaldesi V., Moricone M., Influence of mineral additions on the performance of 100% recycled aggregate concrete., (2009). Construction and Building Materials, v. 23, p. 2869-76.

Tam V.W.Y., Wang K., Tam C.M., (2008). Assessing relationships among properties of demolished concrete, recycled aggregate concrete using regression analysis. Journal of Hazardous Materials, v. 152, p. 703-14.

Tam V.W.Y., Tam C.M., (2008). Crushed aggregate production from centralized combined and individual waste sources in Hong Kong. Construction and Buildings Materials, v. 21, p. 879-86.

Eguchi K., Teranishi K., Nakagome A., Kishimoto H., Shinozaki K., Narikawa M, (2007). Application of recycled coarse aggregate by mixture to concrete construction. Construction and Building Materials, v. 21, p. 1542-51.

Bairagi N.K., Ravande K, Pareek V.K., (1993). Behaviour of concrete with different proportions of natural and recycled aggregates. Resources, Conservation and Recycling, v. 9, p. 109-26.

Gómes-Saberón J.M.V., (2002). Porosity of concrete with substitution of recycled concrete aggregate: An experimental study. Cement and Concrete Research, v. 32, p. 1301-11.

Kumutha R, Vijai K., (2010). Strength of concrete incorporating aggregates recycled from demolition waste. ARPN Journal of Engineering and Applied Sciences, v. 5, n. 5, p. 64-71.

Leite M.B., (2001). Evaluation of mechanical properties of concrete made with recycled aggregates of construction and demolition waste. Doctoral thesis. Porto Alegre. School of Engineering, Federal University of Rio Grande do Sul. 270 p. (in Portuguese).

Larrañaga M.E., (2004). Experimental study on microstructure and structural behaviour of recycled aggregate concrete. Doctoral Thesis. Barcelona. Universitat Politècnica de Catalunya. 230p.

Li X., (2009). Recycling and reuse of waste concrete in china. Part II. Structural behaviour of recycled aggregate concrete and engineering applications". Resources, Conservation and Recycling, v. 53, p. 107-12.

Xiao JZ, Tawana MM, Zhu XH. (2009). Study on recycled aggregate concrete frame joints with method of nonlinear finite element. Key Engineering Materials, v. 417/418, 2009, p. 745-748.

Mehta P.K., Monteiro P.J.M., (2008). Concreto: estrutura, propriedades e materiais. São Paulo: PINI.

Hordijk D.A.,(1991) Local Approach to Fatigue of Concrete. PhD thesis. Delft University of Technology.

Gopalaratnam V.S., Shah S.P., (1985). Softening Response of Plain Concrete in Direct Tension. ACI Journal, p. 310-323.

Hillerborg A., Modeer M., Petersson P.E., (1976). Analysis of crack growth in concrete by means of fracture mechanics and finite elements. Cement and Concrete Research, v. 6, p. 773-82.

NBR 7222, (1994). ABNT – Brazilian Association of Technical Standards: Mortar and concrete – Determination of splitting tensile strength– Method of test. Rio de Janeiro, (in Portuguese).

NBR 12142, (1994). ABNT – Brazilian Association of Technical Standards: Concrete – Determination of flexural tensile strength – Method of test. Rio de Janeiro, (in Portuguese).

Santiago, E.Q.R., (2008). Utilization of aggregates of EVA and CDW to obtaining lightweight concretes. Masters dissertation. State University of Feira de Santana, Feira de Santana. 168 p. (in Portuguese).

Rots J.G., (1988). Computational modeling of concrete fracture. PhD Thesis. Delft University of Technology. 141 p.

Menin R.C.G., Trautwein L.M., Bittencourt T.N. (2009). Smeared Crack Models for Reinforced Concrete Beams by Finite Element Method. Ibracon Structures and Materials Journal, v. 2, p. 166-200 (in Portuguese).

Feenstra P.H., de Borst R., Rots J.G., (1991). A comparison of different crack models applied to plain and reinforced concrete. Fracture Processes in Concrete, Rock and Ceramics, p. 629-638.

DIANA, (2005). User's Manual - Release 9. Last modified Fri Apr 29 13:34:17.

Model Code 1990 – Design Code, (1991). Commite Euro-International du Beton (CEB) & Federation International de la Précontraite (FIP)., Lausanne: Thomas Telford Services Ltd.

Bazant Z.P., Oh B.H., (1983). Crack band theory for fracture of concrete. Materials and Structures, v. 16, n. 93, p. 155-77.

International Organization for Standardization (ISO) 4013, (1978). Concrete – Determination of flexural strength of test specimens.